Electrochemical detection of dopamine using a simple redox cycling-based device

Mustafa ŞEN*

Faculty of Engineering and Arhitechture, Department of Biomedical Engineering, Izmir Katip Çelebi University, İzmir, Turkey

Abstract

Here, a dual ITO microchip was fabricated for high sensitive detection of dopamine (DA) based on redox-cycling. The ITO electrodes with 3×3 mm working areas were made via photolithography and dry etching processes. The microchip was obtained by first aligning the working areas of two ITO electrodes to overlap and then fixing them in that position using a double-sided tape, which also formed a sealed microchannel between the ITO electrodes for test solution delivery. The ITO electrodes and microchips were electrochemically characterized using EIS, cyclic voltammetry and chronoamperometry. Compared to a single ITO electrode in a microchannel, the microchip had a significantly higher signal due to redox cycling. The microchip was lastly used for the detection of DA at varying concentrations. According to the results, the microchip had an LOD of 0.15 µM in a linear detection region of 0.1 to 50 µM. The microchip requires less than 1 µl of solution to complete the analysis and has great potential to be applied for immunosensing.

Keywords: *Redox-cycling, dopamine, ITO microchip, electrochemical measurement, microfabrication*

1. Introduction

Dopamine (DA) is a neurotransmitter that plays an important role in the cardiovascular and central nervous systems. Therefore, high DA levels indicate cardiotoxicity leading to rapid heartbeat, hypertension and heart failure. On the contrary, low DA levels in the central nervous system are seen as the main cause of various neurological diseases such as Parkinson's disease, schizophrenia, Alzheimer's disease, stress and depression [1]. Therefore, it is clear that DA measurements are necessary to understand its biological functions and related biological processes/mechanisms. Currently, there is a growing interest in developing specific and low-cost biosensors that take advantage of the ease with which DA is oxidized on an electrode surface. In addition, the biosensors should be able to provide a sensitive response in the appropriate concentration range (0.01–1 µM for a healthy individual and in the nanomolar range for patients with Parkinson's disease) [2]. In this study, sensitive detection of DA was performed with a dual ITO microchip that can amplify the signal based on redox cycling. The 3×3 mm working areas of two ITO microchips were designed to overlap with the help of double-sided tape, and a dual ITO microchip was created with a microchannel. The applicability of the dual ITO microchip as a biosensor was analyzed using different concentrations of DA solution.

2. Materials and Methods

2.1. Materials

DA hydrochloride (SigmaAldrich, USA), phosphate buffered saline (PBS - 0.01 M phosphate buffer, 0.0027 M KCl and 0.137 M NaCl, pH 7.4 at 25 °C), potassium ferricyanide ($K_3Fe(CN)_6$) (Sigma-Aldrich, USA), potassium ferrocyanide ($K_4Fe(CN)_6$) (Sigma-Aldrich, USA), $FcCH_2OH$) (Sigma-Aldrich, USA), Multi-potentiostat (µStat-i 400 (Bi)potentiostat/Galvanostat/Impedance Analyzer (EIS), DropSens Metrohm, Switzerland)

2.2. ITO microfabrication

Microchips were produced from indium tin oxide (ITO) films using the “ion-beam etching” process. Firstly, the surfaces of ITO coated glass substrates (slides) were cleaned with the help of distilled water and acetone. Next, cleaned ITO-coated glasses were placed in the “Spin-Coater” device and coated with “AZ5214E” (MicroChemicals, Germany) positive/reversal photoresist to cover the entire surface. The coating process was carried out at 2000 rpm for 60 s. Afterwards, the slides covered with photoresist were kept in an oven set at 90 °C for 30 minutes to ensure the polymerization (pre-baking) of the photoresist. A lithography mask with the desired design was used to transfer the patterns to the microchip. Briefly, the patterns on the mask were exposed

*Corresponding author. *e-mail address: mustafa.sen@ikc.edu.tr*

to UV light via a UV mask aligner and transferred onto photoresist-coated slides [3]. An alkaline developer was used to remove the areas exposed to UV light. Afterward, etching process was carried out with the help of "ion beam etching" device with 30 sccm Argon gas for 1 hour using the parameters 750 V, 49 W, 0.05 A and the sample holder was rotated at an angle of 22.5°.

2.3. Electrochemical characterization with electrochemical impedance spectroscopy (EIS)

EIS measurements of ITO microchip were performed in 50 mM $[Fe(CN)_6]^{3-/4-}$ + 0.1 M KCl solution. Impedance spectra were recorded at open circuit potential with a 10 mV amplitude signal in the frequency range of 10 Hz to 10 kHz [4,5]. R_{ct} values were calculated with fit and simulation option in AUTOLAB 302 Nova 2.1.5 software using Randles circuit model.

2.5. Redox-cycling

The 3×3 mm working areas of two ITO microchips were aligned to overlap and then fixed using a double-sided tape to form a sealed microchannel. Electrochemical characterization of the dual ITO microchip was carried out using cyclic voltammetry (CV) and chronoamperometry. Briefly, the microchannel was first filled with 200 µM DA and 0.1 mM $FcCH_2OH$, respectively [6]. Then the generator electrode was scanned from 0 V to +0.35 V (vs. Ag/AgCl) at a scanning rate of 0.05 V/s, while the collector electrode was fixed at 0 V (vs. Ag/AgCl) in a dual mode measurement where redox cycling was induced. The applicability of the dual ITO microchip was demonstrated with DA solutions at different concentrations (0, 0.01, 0.05, 0.1, 0.5, 1, 10, 50, 100 µM). Basically, the generator and collector electrodes were set at +0.35 V and 0 V (vs. Ag/AgCl) for 50 s and the oxidation and reduction currents at 50 s were used to obtain a calibration curve. The limit of detection (LOD) was calculated based on three replicates using the following equation: LOD = 3.3 × (standard deviation of the calibration curve/slope of the calibration curve)[7,8]. All electrochemical experiments were performed using a multi-potentiostat.

3. Results and Discussion

Using the proposed fabrication method, the 3×3 mm working areas of two ITO microchips were successfully and correctly overlapped using a double-sided tape and a microchannel was formed for test solution delivery. In other words, the fabrication of a dual ITO microchip was realized using a simple fabrication procedure without using laborious and precise alignment processes. The electrochemical behavior of a single ITO was analyzed by CV using 0.1 mM $FcCH_2OH$ and 200 µM DA, as shown in Figure 1a-b. The CV curves as expected confirmed the electrochemical detection of $FcCH_2OH$ and DA. As can be seen in the Nyquist plot of ITO, the R_{ct} value was measured to be 590 Ω (Figure 1c).

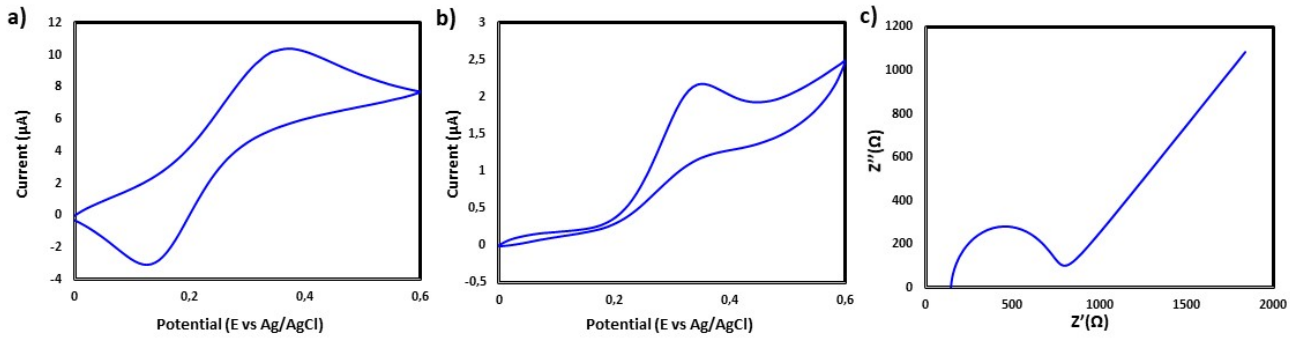

Figure 1. CV curves of bare ITO recorded in 0.1 mM $FcCH_2OH$ (a) CV curves of bare ITO recorded in 200 µM DA (b) EIS curves of bare SPCE (c)

In dual-mode chronoamperometry, redox-cycling capacity of a dual ITO microchip was studied by first setting the potential of both the generator and collector electrodes first at +0.35V (vs. Ag/AgCl) and then +0.35 and 0 V (vs. Ag/AgCl), respectively (Figure 2a). When the two electrodes were set at +0.35V (vs. Ag/AgCl), both electrodes oxidize and consume $FcCH_2OH$ in the microchannel, resulting a low current (0.08 µA). However,

when the generator and collectors were set at +0.35 and 0 V (vs. Ag/AgCl), respectively, the generator electrode oxidizes $FcCH_2OH$ to $FcCH_2OH^+$ which is then reduced back to $FcCH_2OH$ by the collector electrode. Thus, a redox-cycling is induced, resulting a much higher current (3.1 µA). Figure 2b shows the behavior of dual-mode CV curves at different scanning rates in 0.1 mM $FcCH_2OH$.

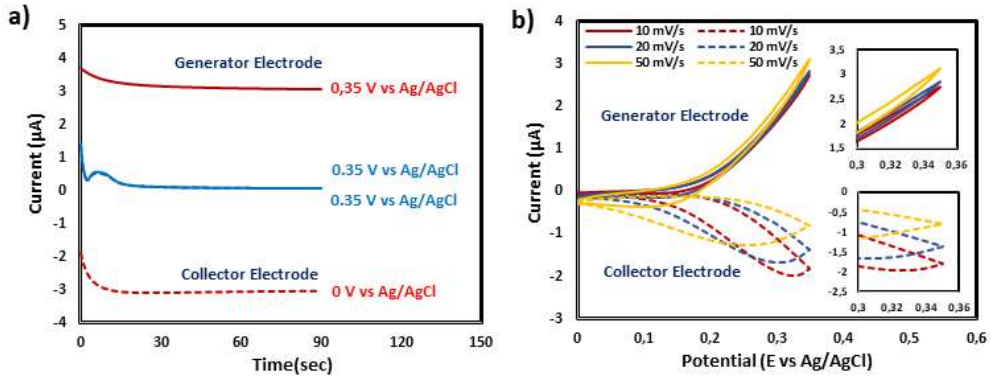

Figure 2. Dual mode chronoamperometry from dual ITO in 0.1 mM $FcCH_2OH$ at different potential (a) dual mode cyclic voltammograms from dual ITO in 0.1 mM $FcCH_2OH$ at different scan rates (b).

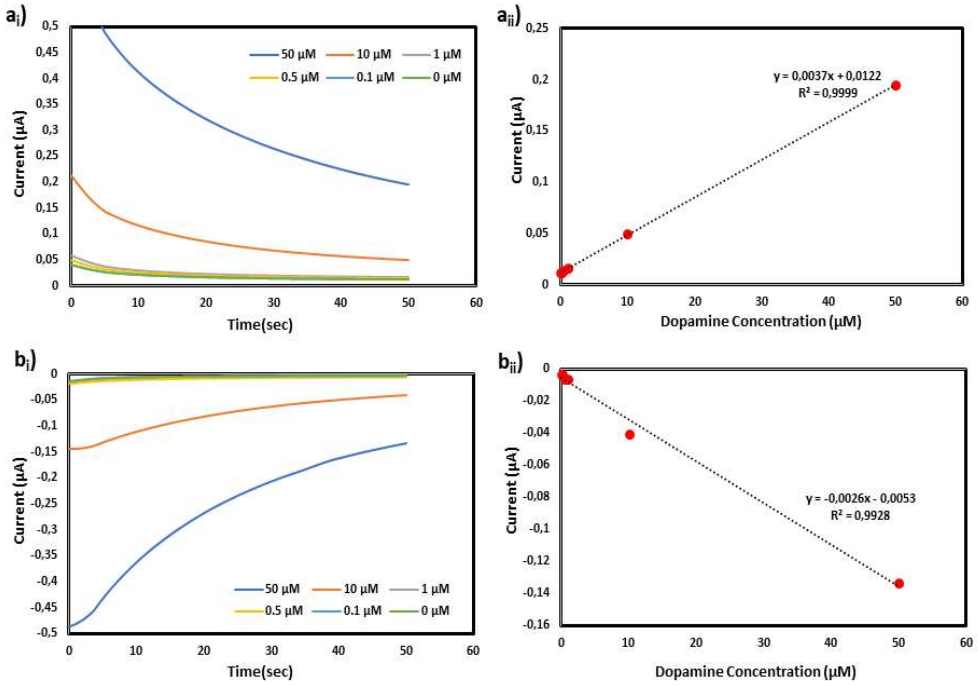

Figure 3. Chronoamperometric curves obtained in PBS with varying concentration of DA (0, 0.1, 0.5, 1, 10 and 50 µM) oxidation curve (a_i) reduction curve (b_i) and a calibration curve obtained based on the last oxidation current (a_{ii}) and a calibration curve obtained based on the last reduction current (b_{ii}).

The performance of the dual ITO microchip for the detection of DA was evaluated in dual mode. Basically, the potentials of generator and collector electrodes were set at +0.35 and 0 V (vs. Ag/AgCl), respectively, as described above. As the DA is oxidized to DA quinone (DAQ) by the generator electrode, DAQ then diffuses to the collector electrode surface where it is reduced back to DA, resulting signal amplification and a higher current. Figure a_i-b_i show the oxidation and reduction-based choronoamperometric responses obtained in DA solutions at varying concentrations, respectively. In both cases, the currents at 120s were used to obtain calibration curves (Figure a_{ii}-b_{ii}). The both calibration curves had an R^2 value greater than 0.99. The LOD values for the generator

and collector electrodes were calculated to be 0.15 and 1.46 µM, respectively. The microchip requires less than 1 µl of solution for analysis and can be applied for immunosensing with enzymes producing molecules that can be electrochemically cycled between two electrodes.

Acknowledgment

This research was supported by the scientific research projects coordination unit of Izmir Katip Celebi University (Project Nos. 2022-ÖDL-MÜMF-0007 and 2021-GAP-MÜMF-0055).

References

[1] Klein, M.O., Battagello, D.S., Cardoso, A.R., Hauser, D.N., Bittencourt, J.C., Correa, R.G., (2019). Dopamine: functions, signaling, and association with neurological diseases. *Cell. Mol. Neurobiol.*, 39, 31–59.

[2] Lakard, S., Pavel, I.-A., Lakard, B., (2021). Electrochemical biosensing of dopamine neurotransmitter: A review. *Biosensors*, 11, 179.

[3] Şen, M., Ino, K., Ramón-Azcón, J., Shiku, H., Matsue, T., (2013). Cell pairing using a dielectrophoresis-based device with interdigitated array electrodes. *Lab a Chip*, 13, 3650-3652.

[4] Seven, F., Gölcez, T., Mustafa, Ş.E.N., (2020). Nanoporous carbon-fiber microelectrodes for sensitive detection of H2O2 and dopamine. *J. Electroanal. Chem.*, 864, 114104.

[5] Şen, M., (2019). Using electropolymerization-based doping for the electroaddressable functionalization of a multi-electrode array probe for nucleic acid detection. *Anal. Sci.*, 35, 565–569.

[6] Şen, M., Ino, K., Shiku, H., Matsue, T., (2012). Accumulation and detection of secreted proteins from single cells for reporter gene assays using a local redox cycling-based electrochemical (LRC-EC) chip device. *Lab a Chip*, 12, 4328-4335.

[7] Mercan, Ö.B., Kılıç, V., Şen, M., (2021). Machine learning-based colorimetric determination of glucose in artificial saliva with different reagents using a smartphone coupled µPAD. *Sensors Actuators B Chem.*, 329, 129037.

[8] Şen, M., Azizi, E., Avcı, İ., Aykaç, A., Ensarioğlu, K., Ok, İ., Yavuz, G.F., Güneş, F., (2022). Screen printed carbon electrodes modified with 3D nanostructured materials for bioanalysis. *Electroanalysis*, 34, 1-10.

English Title (Identification of potent COVID-19 ...) (times new roman 14 bold)

Name SURNAME[1,*], Name SURNAME[2], Name SURNAME[3] ***(times new roman 11 bold-italic)***

[1]Institute, Faculty, Department, University, City, Country ***(times new roman 9 italic)***

[2]Institute, Faculty, Department, University, City, Country ***(times new roman 9 italic)***

[3]Institute, Faculty, Department, University, City, Country ***(times new roman 9 italic)***

Abstract

In this study, the relationship between transport performance of Cr(VI) through PVDF-co-HFP based ionic polymer inclusion membranes (IPIM), alkyl chain length of symmetric imidazolium bromide based room temperature ionic liquids (RTILs), and morphological changes of these IPIMs has been comprehensively described. Butyl, hexyl, octyl, and decyl substituted RTILs containing IPIMs were prepared in different compositions and their effectiveness on Cr(VI) transport was experimentally optimized. In optimum conditions, the initial mass transfer coefficient (J_o) value of Cr(VI) was found as $5.0x10^{-6}$ $mols^{-1}m^{-2}$, and also, we found that the optimized process is significantly selective for chromium in existence the other heavy metal ions. Morphological and structural characterizations of IPIMs have been performed before and after Cr(VI) transport to illuminate the morphological and structural changes. Also, the additional plasticizing effect of RTILs as an unusual morphological phenomenon has come forward. In today's industrialised world, the demand for environmentally friendly processes for removal or recycle of toxic substances by simpler and cheaper ways have been increasing day by day. As a result, our developed and optimised membrane-based process seems to be overcome some Cr(VI) dependent environmental and industrial difficulties. **(times new roman 10) (75-300 words)**

Keywords*(max.5)*: *Keyword1, Keyword2, Keyword3, Keyword4, Keyword5* ***(times new roman 10)***

Total page number should be max six(6) pages.

1. Introduction (times new roman 12 bold)

In the world, each pollution types, existing in different environmental sources, affects a significant amount of the organisms who live in there [1-3]. The discharge limits of heavy metals at the end of the industrial activities should be held in the acceptable concentration limits according to the boundaries of World Health Organization (WHO) and EPA [4, 5]. The high-level intake or exposure to the chromium can create bad results on survival conditions of humans, animals and plants depending on the chromium species [6, 7]. Cr(III) in lower concentrations has less toxic than Cr(VI) on natural life. Cr(III) especially shows its toxic effects on the viscera of mammal organisms like liver and kidney [8-10]. (times new roman 11) References should be given in order.

$$E = mc^2 \quad \text{(times new roman 11)} \qquad (1)$$

In the present study, we aimed to illuminate Cr(VI) transport through PVDF-co-HFP based IPIMs by using RTILs involving different lengths of alkyl chains. For this purpose, butyl, hexyl, octyl, and decyl substituted RTILs were synthesised and characterised using spectral and physicochemical characterization techniques like NMR, viscosity measurement, electrical conductivity, density, refractometry, etc.

2. Materials and Methods(times new roman 12 bold)

2.1. Apparatus (times new roman 11 bold)

The reagents, 1H-imidazole, 1-bromo propane, 1-bromo hexane, 1-bromo octane and 1-bromo decane, employed in the synthesis of RTILs and were purchased from VWR (Seelze, Germany) and used directly in the RTIL synthesis without further purification. Dichloromethane, toluene, diethyl ether, hexane, N,N-dimethyl formamide, NH_4OH, Na_2CO_3, KOH, HCl, HNO_3, NaOH, and H_2SO_4 were purchased from Sigma-Aldrich (Sleaze, Germany) and used directly without any purification.

3. Results and Discussion(times new roman 12 bold)

3.1. Selection of working wavelength (times new roman 11 bold)

We have illuminated the usage of imidazolium-based RTILs having different lengths of alkyl chains in symmetric positions as carrier in PVDF-co-HFP based PIMs as a carrier.

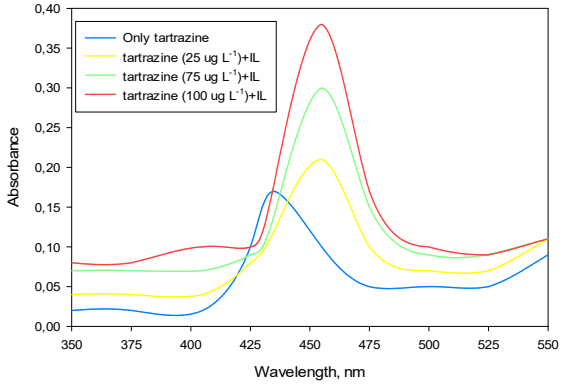

Figure 1. Absorbance spectra obtained in selected chemical conditions. (times new roman 10)

3.2. Effect of pH

Electrostatic interactions between chemical species vary depending on the pH of the aqueous solution. In the extraction experiments, the interaction between the analyte and the selected chemical medium should be high.

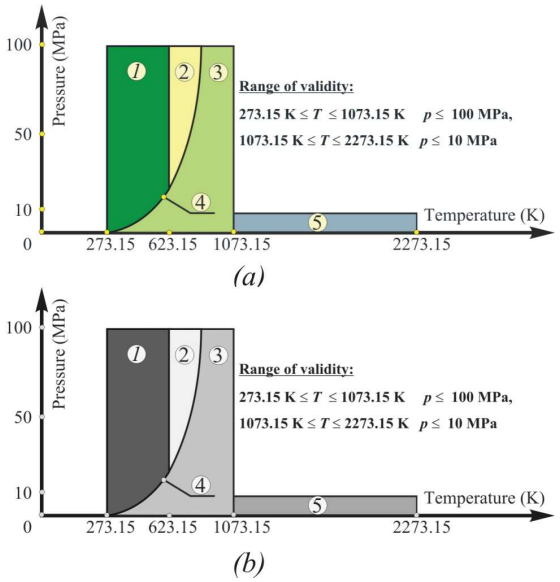

Figure 2. Use of appropriately contrasting colours for black and white printing: a) colour figure, b) greyscale figure.

Table 1. Table format in IKSTC: Template for manuscripts. **(times new roman 10)**

Interfering species	Tolerance limits	Recovery (%)	RSD (%)
Sn^{2+}	1000	94.7	2.1
Cd^{2+}	1000	96.4	2.4
K^{+}	1000	98.1	2.2
Co^{2+}	1000	95.3	2.1
Mg^{2+}	1000	96.2	2.0
Ca^{2+}	750	96.8	2.8
Tartaric acid	750	97.5	2.5
Ponceau 4R	750	96.5	2.6
Fe^{3+}	750	98.2	1.8
SO_4^{2-}	500	94.4	2.7
Allura red AC	500	95.9	2.5
Ascorbic acid	500	97.1	2.6
Al^{3+}	500	96.3	2.9
Brilliant Blue	250	96.5	2.5
Sunset yellow	250	93.4	2.4

Erythrosine	250	93.1	2.1
Carmoisine	100	92.4	2.8
Amaranth	100	92.5	2.5

**footnote and abbreviation times new roman 9 punto

Acknowledgment

In this study, the financial support was provided by The Scientific and Technological Research Council of Turkey (TUBITAK), Project No. 112T806. All experimental works were conducted in Çankırı Karatekin University Research Laboratory. The author would like to thanks to all supporters due to their precious contributions.

References (Max.40) (times new roman 12 bold) *Journal name should be written in italics (journals)* (times new roman 11)

[1] Nosrati, S., Jayakumar, N. S., Hashim, M. A., & Mukhopadhyay, S. (2013). Performance evaluation of vanadium (IV) transport through supported ionic liquid membrane. *Journal of the Taiwan Institute of Chemical Engineers*, *44*(3), 337-342.

[2] Soylak, M., & Yilmaz, E. (2011). Ionic liquid dispersive liquid–liquid microextraction of lead as pyrrolidinedithiocarbamate chelate prior to its flame atomic absorption spectrometric determination. *Desalination*, *275*(1-3), 297-301.
(for book chapters) (times new roman 11)

[3] Murdock, T. A., Veras, E. F., Kurman, R. J., & Mazur, M. T. (2018). *Diagnosis of endometrial biopsies and curettings: A practical approach*. 2nd ed. Berlin: Springer, 100-120.
(for book)

[4] García-Río, E., & Kupeli, D. N. (2013). *Semi-Riemannian maps and their applications* (Vol. 475). Springer Science & Business Media.
(for websites)

[5] National Cancer Institute, Surveillance Epidemiology and End Results. Cancer of the Corpus and Uterus, NOS. Available at: http://seer.cancer.gov/statfacts/html/corp.html?statfacts_page=corp. Retrieved March 2, 2008.
(thesis)

[6] Surname N., Title of thesis, PD or master thesis, Name of university, name of institue, year.
(Abstratcs in conferences are not accepted as a valid reference except full text)

[7] Surname N., Title of fulltext conference paper, name of conference, city, year, pages.